

# Seismic pursuit of wormholes

LARRY LINES, SANDY CHEN, P. F. DALEY, and JOAN EMBLETON, University of Calgary, Canada  
LARRY MAYO, EnCana Corporation, Calgary, Alberta, Canada

Cold production has become increasingly popular in the extraction of heavy oil, due to the development and widespread use of progressing cavity pumps—essentially powerful augers that suck both oil and sand into the well. At the onset of production, these pumps produce about 60% oil and 40% sand. However, production can improve to 95% oil with only 5% sand after a few months. This increase in oil production and reduction in sand production is attributed to the development of high-porosity tubes termed “wormholes.” Roche (2002) describes wormhole development as the creation of a network of “horizontal wells without using a drilling rig.” Operators who plan infill drilling rely on wormhole distribution information to optimize well spacing. It is accepted that aggressive cold production of oil sands will increase oil recovery, and this has been demonstrated in several pools, both in Alberta and Saskatchewan.

So, assuming these induced sand channels can boost cold heavy oil production, can we map them? That’s a good question because wormholes have small dimensions compared to seismic wavelengths, making their seismic detection extremely difficult. This challenge caused us to perform feasibility tests based on a number of models from the literature. The following describes the results of these tests. We also show some real seismic data with promising indications for wormhole imaging.

**Background.** Much heavy oil recovery in Western Canada involves steam injection. Time-lapse seismology plays a major role in monitoring steam fronts and time-lapse or “4D seismology” is now a standard reservoir characterization tool.

However, steam production/injection is costly, and heavy oil production now increasingly uses cold flow techniques. As stated earlier, cold production methods use special pumps, known as progressing cavity pumps (Figure 1). These pumps, similar to an auger or “Archimedes screw” within a flexible sleeve, lift the oil/sand mixtures from the producing formation to the surface. The removal of quantities of oil/sand from the reservoir creates a region of low pressure in the vicinity of the well that allows an oil/sand flow from within the reservoir to the well. It has been determined that this transport process occurs through the formation of tubes of high-porosity sandstone or wormholes which, as shown by Tremblay et al. (1999), can have porosities that exceed 50%!

Figure 2 shows that wormhole patterns have a fractal-like nature similar to root systems or tree branches. Wormholes have been created in the reservoir simulation laboratories at the Alberta Research Council. Figure 3, CT scans of these wormhole tubes, shows that their diameters are often about 10 cm, although Tremblay suggests that they could be as large as 1 m. These dimensions are far less than what can realistically be resolved by surface seismic.

However, if we consider the imaging problem from a macroscopic perspective, location of individual wormholes is not the major concern. Seismic recognition of regions of high concentrations of wormholes may be just as valuable for field development and such a region of the reservoir may be visible via standard reflection techniques as a consequence of the change in elastic parameters brought about by the existence of wormholes.

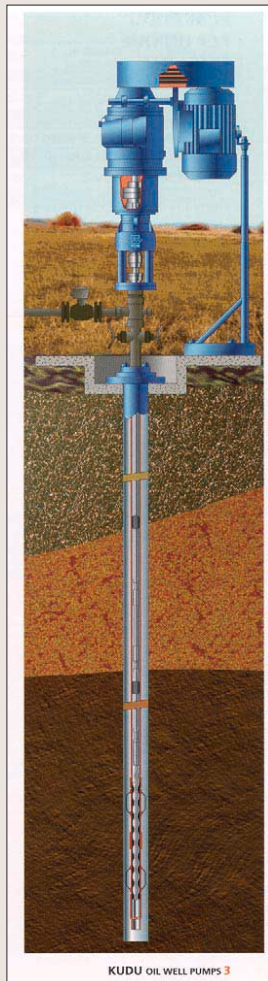


Figure 1. A schematic of a cold production oil pump (courtesy of Kudu Oil Well Pumps).

**Methodology and results.** According to Tremblay et al., wormholes will typically be tens of centimeters in diameter but can extend for distances of 100-200 m. As shown by Figure 3, the small size of wormholes compared to normal seismic wavelengths will make seismic detection very challenging—if not impossible. In order to test the feasibility of seismic in this situation, we analyzed various wormhole models. In particular, we examined the seismic frequencies needed for detection and the response of wormhole models for normal seismic frequencies.

Our first wormhole model was based largely on the chaotic fractal-like model described by Yuan et al. (1999). The model (Figure 4) was obtained by using random paths with branching. The random steps have a slight horizontal bias with some branching of wormhole paths. The path randomness is similar to the model shown by Yuan et al. The thickness of wormhole tubes was 10 cm for a model with dimensions of 60 × 60 m. Seismic velocity for the wormholes (50% porosity) is 1875 m/s. Seismic velocity for the surrounding oil sands (38% porosity) is 2030 m/s. The velocities are derived using Wyllie’s equations.

The exploding-reflector seis-

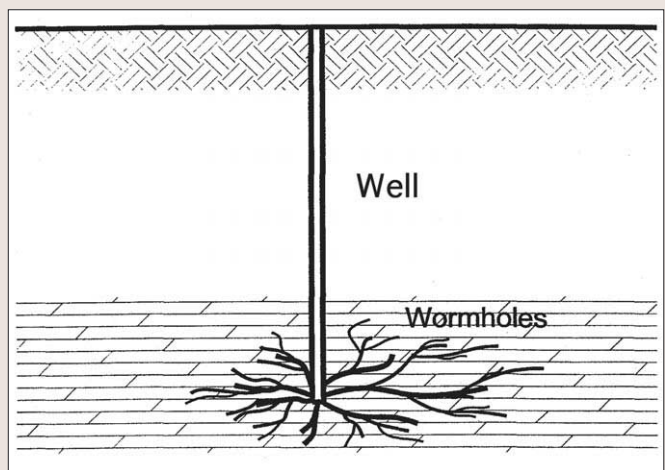


Figure 2. A schematic of a wormhole model as shown by Miller et al. (1999).

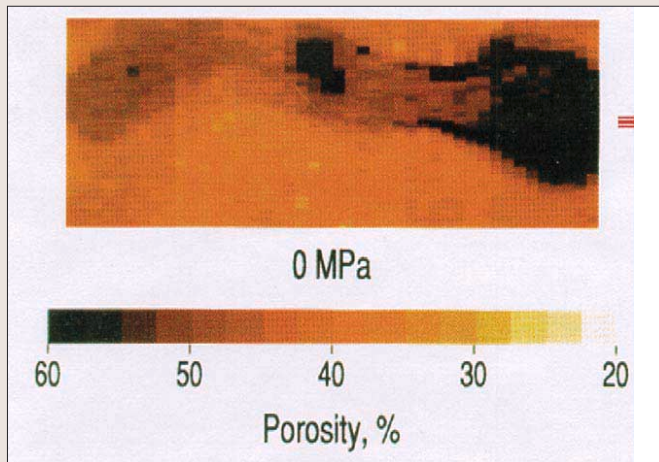


Figure 3. The above CT scan of wormhole (with width of 10 cm) was shown by Tremblay et al. (1999).

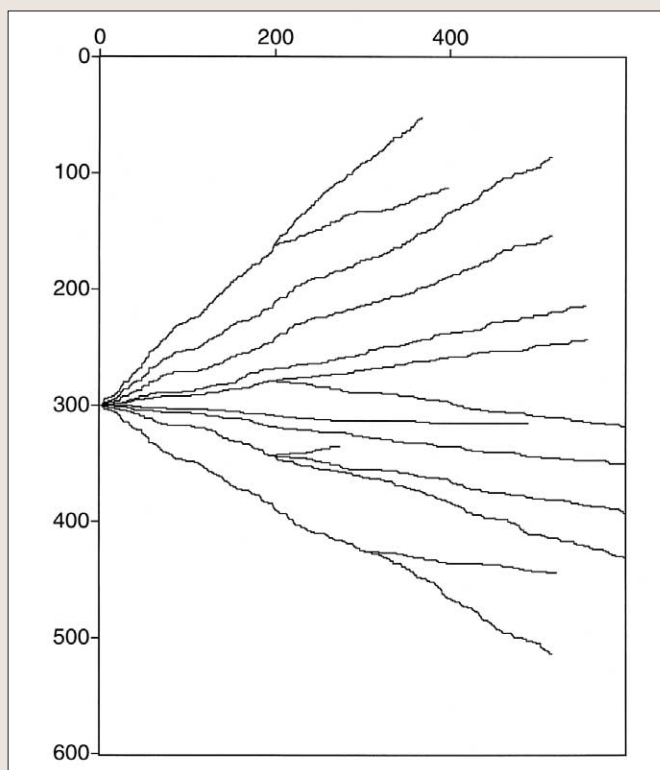


Figure 4. The chaotic wormhole model of dimensions  $60 \times 60$  m was used in modeling tests.

mogram in Figure 5 was computed for a seismic wavelet with a dominant frequency of 3000 Hz. Individual wormholes can be detected with these extremely high frequencies. However, it would be unusual to see such high frequencies in field data (except possibly in cross-borehole seismology), so we adjusted our analysis to more realistic frequencies. Figure 6 shows that, when the seismogram is bandpassed to a peak frequency of 750 Hz, reflections merge together. Further bandpassing the data to a more realistic peak frequency of 185 Hz results in a blurred image (Figure 7). Therefore, we conclude that, unless we have incredibly high frequencies, we would be unable to detect individual wormholes.

This caused us to consider, instead of imaging individual wormholes, detecting wormhole presence. Wormholes can create connectivity within the reservoir and can extend for 100-250 m. Thus, if enough wormholes exist, the porosity of the producing oil sands should affect the seismic response. If we

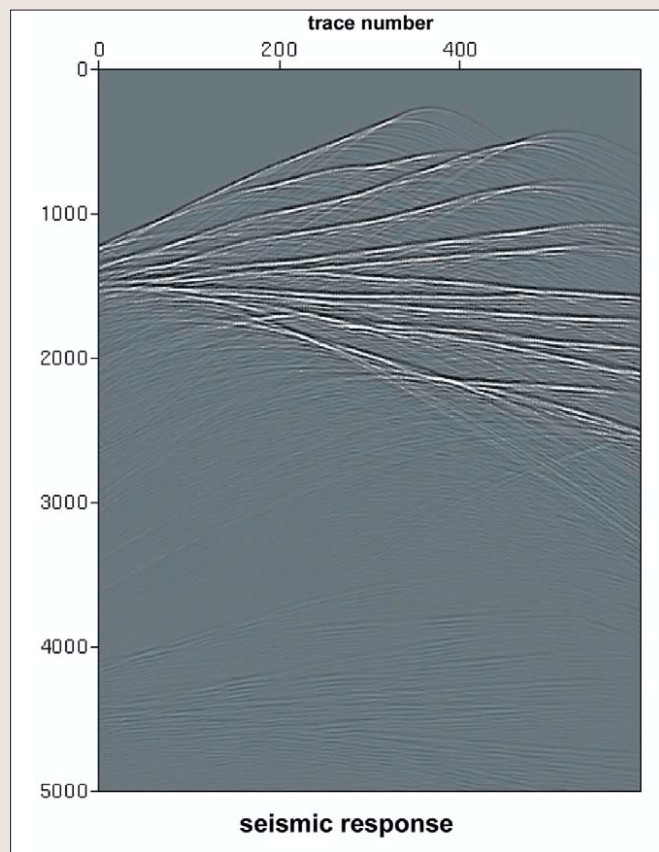


Figure 5. Synthetic seismogram for the model in Figure 4 with ultrahigh frequency data. The temporal sample interval on the vertical axis is .010 ms and the trace spacing is 10 cm. (Plot dimensions are  $60 \text{ m} \times 50 \text{ ms}$ .)

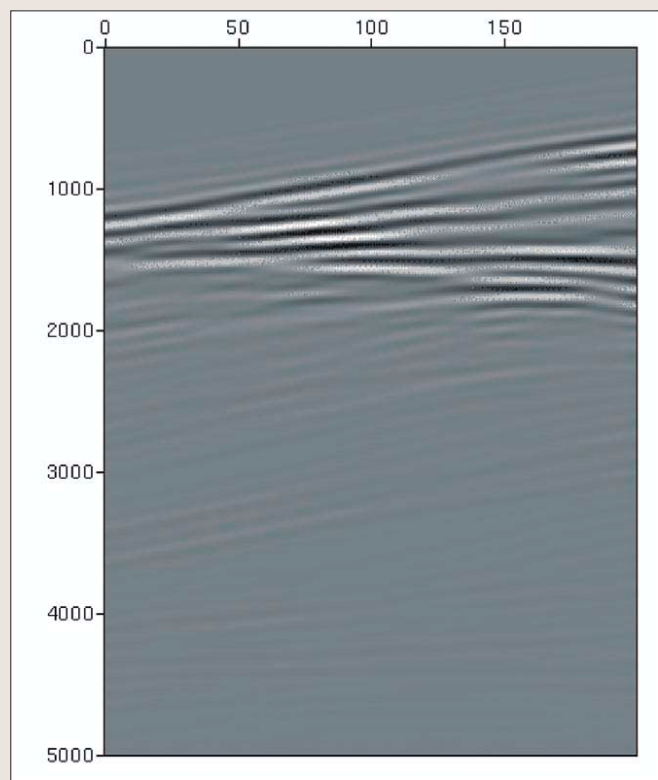


Figure 6. Synthetic seismogram for left 20 m of previous model bandpassed to 750 Hz.

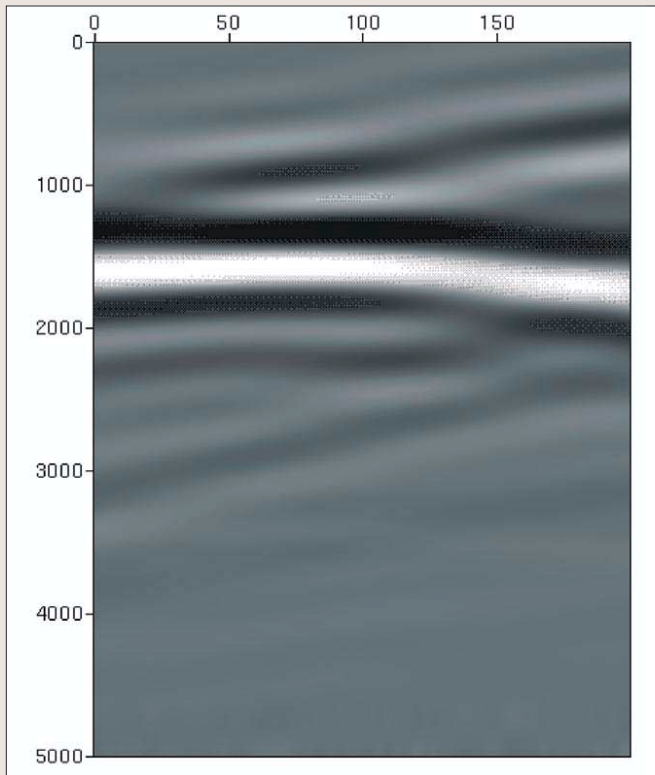


Figure 7. Synthetic seismogram of Figure 6 bandpassed to peak frequency of 185 Hz.

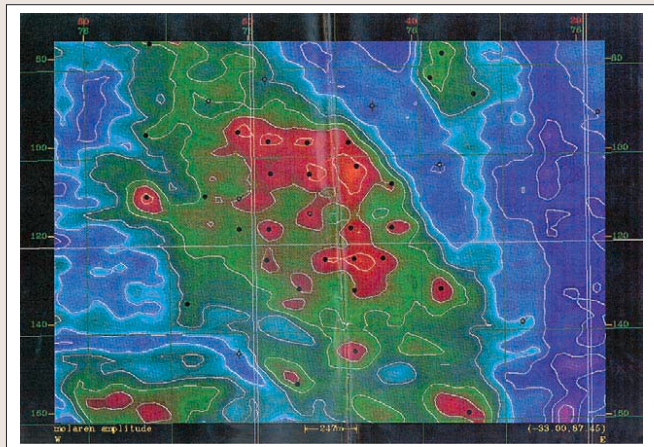


Figure 8. Map of seismic amplitudes from Mayo (1996) shows a series of anomalies centered around the well sites. These are believed related to wormhole development in cold production.

examine the seismic response before and after (during) the production of oil sands, then merely differencing the seismograms may illuminate wormhole development. Since Figure 7 showed that a seismic response will result from the integrated effect of wormholes on the seismic signature, we will be attempting further model testing using well logs and seismic data.

**Possible wormhole effects on field data.** Although most seismic wormhole detection efforts have been in numerical modeling or laboratory simulations, the case history presented by Mayo (1996) may indicate that wormholes can create a seismic effect.

Attention was focused on this possibility when it was noticed that seismic amplitude anomalies were centered around cold production wells (Figure 8). The seismic anomalies may have been caused by the production process. The

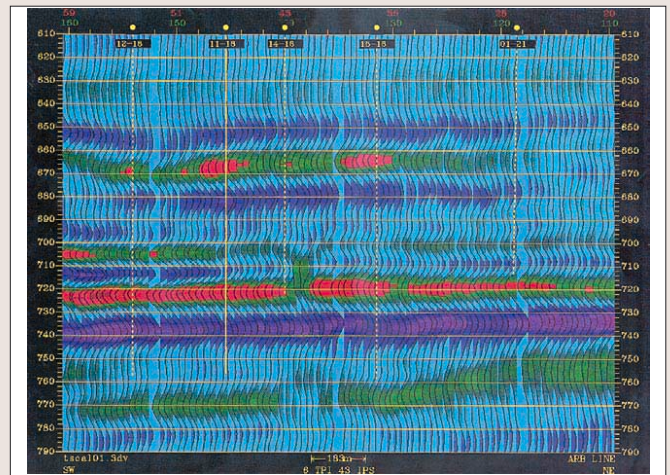


Figure 9. This seismic section showed an increase in the amplitude of negative troughs between 660 and 670 ms in the oil-sand zones. These amplitude changes are located at the four wells on the section that have undergone cold production.

seismic line in Figure 9 shows an increase in amplitude at the reservoir level near the wells. These large negative troughs were caused by a lowering of the seismic impedance—possibly due to the existence of wormholes. However, it is still not clear if the effect on the seismic signature and the lowered acoustic impedance is primarily due to the increased porosity or to the creation of foamy oil. Foamy oil, which has a texture not unlike shaving cream, is caused by depressurization of gas-saturated heavy oil. This depressurization increases the total fluid volume, forcing gas and oil into borehole. The combined effects of porosity and foamy oil in wormholes will be studied in future modeling experiments.

**Conclusions and future directions.** Our modeling studies demonstrate that seismic detection of individual wormholes is not feasible. However, the presence of many high-porosity wormholes could alter medium properties sufficiently to manifest a seismic response. The important issue is that wormholes will increase the porosity and thereby decrease the seismic velocity. Therefore, time-lapse seismic monitoring methods may also apply to heavy oil cold flow production. This has been supported by real data from areas of possible porosity development and foamy oil production. Further modeling and research on real data is needed to quantify the seismic effects of wormholes.

**Suggested reading.** “Seismic monitoring of foamy heavy oil, Lloydminster, Western Canada” by Mayo (SEG Expanded Abstracts, 1996). “Air injection recovery of cold-produced heavy oil reservoirs” by Miller et al. (presented at the CIPC Conference of the Petroleum Society in Calgary, 2001). “Wormholes” by Roche (Nickles New Technology Magazine, 2002). “CT imaging of wormhole growth under solution-gas drive” by Tremblay et al. (SPE Reservoir Evaluation & Engineering, 2, paper 54658, 1999). “Heavy-oil reservoir characterization using elastic wave properties” by Watson et al. (TLE, 2002). “A wormhole network model of cold production in heavy oil” by Yuan et al. (SPE symposium in Bakersfield, California, paper 54097, 1999). **TJE**

*Acknowledgments:* We thank COURSE Project #1445 for funding. We also thank Alberta Research Council and Husky Energy for their scientific input for this project.

Corresponding author: lines@geo.ucalgary.ca